

Trilinear Gauge Boson Vertices in the MSSM

A. B. Lahanas [†] and V. C. Spanos [‡]

University of Athens, Physics Department, Nuclear and Particle Physics Section,
Ilissia, GR – 15771 Athens, GREECE

Abstract

We study the C and P even $WW\gamma$ and WWZ trilinear gauge boson vertices (TGV's), in the context of the MSSM as functions of the soft SUSY breaking parameters $A_0, m_0, M_{1/2}$ and the momentum q carried by γ, Z , assuming the external W 's are on their mass shell. We follow a complete renormalization group analysis taking into account all constraints imposed by the radiative breaking of the electroweak symmetry. It is found that for energies $\sqrt{s} \equiv q^2 \leq 200 \text{ GeV}$ squark and slepton contributions to the aforementioned couplings are two orders of magnitude smaller than those of the Standard Model (SM). In the same energy range the bulk of the supersymmetric Higgs corrections to the TGV's is due to the lightest neutral Higgs, h_0 , whose contribution is like that of a Standard Model Higgs of the same mass. The rest have negligible effect due to their heaviness. The contributions of the Neutralinos and Charginos are sensitive to the input value for the soft gaugino mass $M_{1/2}$ being more pronounced for values $M_{1/2} < 100 \text{ GeV}$. In this case and in the unphysical region, $0 < \sqrt{s} < 2M_W$ their contributions are substantially enhanced resulting to large corrections to the static quantities of the W boson. However such an enhancement is not observed in the physical region and their corrections to the TGV's are rather small. In general for $2M_W < \sqrt{s} < 200 \text{ GeV}$ the MSSM predictions differ from those of the SM but they are of the same order of magnitude. Deviations from the SM predictions to be detectable require sensitivities reaching the per mille level and hence unlikely to be observed at LEP200. For higher energies SM and MSSM predictions exhibit a fast fall off behaviour, in accord with unitarity requirements, getting smaller by almost an order of magnitude already at energies $\sqrt{s} \approx .5 \text{ TeV}$. At these energies the task of observing deviations from the SM predictions, which are due to supersymmetry, becomes even harder requiring higher accuracies.

Athens University
UA/NPPS-18, April 1995

E-mail: [†] alahanas@atlas.uoa.ariadne-t.gr , [‡] vspanos@atlas.uoa.ariadne-t.gr

1. Introduction

The Standard Model (SM) has been remarkably successful in describing particle interactions at energies around the $\sim 100 GeV$. Precise measurements at LEP provided accurate tests of the standard theory of electroweak interactions [1, 2] but we are still lacking a direct experimental confirmation of the non-abelian structure of the standard theory. The $WW\gamma$, WWZ and $ZZ\gamma$ couplings are uniquely determined within the context of the SM and such couplings will be probed in the near future with high accuracy. The study of the trilinear gauge boson vertices (TGV's) in the $e^+e^- \rightarrow W^+W^-$ process is the primary motivation for the upgrading of LEP200 [3] and the potential for measuring these has been discussed in detail [3, 4]. At an energy of about $190 GeV$ and with integrated luminosity of $500 pb^{-1}$ an accuracy of .1 for the determination of these couplings can be obtained. So far there are no stringent experimental bounds on these couplings [5] and the efforts of the various experimental groups towards this direction are still continuing. In the near or remote future with the proposed or already under construction high energy colliders (LHC, NLC, CLIC, JLC) further improvements on the TGV's bounds will be obtained reaching accuracies $\mathcal{O}(10^{-2} - 10^{-3})$ [6]. Such precise measurements are of vital importance not only for the SM itself but also for probing new physics which opens at scales larger than the Fermi scale.

The gauge boson vertex has been the subject of an intense theoretical study the last years. In particular the WWV vertex ($V = \gamma$ or Z) has been analysed in detail within the framework of the standard theory, as well as in extension of it, and its phenomenology has been discussed. The lagrangian density describing the WWV interaction is given by [7, 8]

$$\mathcal{L}^{WWV} = -ig_{WWV}[(W_{\mu\nu}^\dagger W^{\mu\nu} - h.c.) + \kappa_V W_\mu^\dagger W_\nu F^{\mu\nu} + \frac{\lambda_V}{M_W^2} W_{\lambda\mu}^\dagger W_\nu^\mu V^{\nu\lambda} + \dots], \quad (1)$$

$$g_{WWV} = \begin{cases} e & \text{for } V = \gamma \\ e \cot \theta_W & \text{for } V = Z \end{cases}$$

where the ellipsis stand for P or C odd terms and higher dimensional operators. In Eq. (1) the scalar components for all gauge bosons involved have been omitted, that is $\partial \cdot W = \partial \cdot V = 0$, since essentially they couple to massless fermions¹. At the tree level κ_V and λ_V have the values $\kappa_V = 1$, $\lambda_V = 0$. However radiative corrections modify these, the order of magnitude of these corrections being $\mathcal{O}(\frac{\alpha}{\pi}) \sim 10^{-3}$. Sensitivity limits of this order of magnitude will not be reached at LEP200 but can be achieved in future colliders where the TGV's can be studied in detail and yield valuable information not only for the self consistency of the SM but also for probing underlying new physics. Any new dynamics whose onset lies in the TeV range modifies κ_V , λ_V and deviations from the SM predictions are expected.

Supersymmetry (SUSY), is an extension of the SM which is theoretical motivated but without any experimental confirmation. The only experimental hint for its exis-

¹For on shell W 's we have $(\square + m_W^2)W_\mu = 0$ and certainly $\partial \cdot W = 0$, while for the photon $\partial \cdot A$ vanishes on account of current conservation.

tence derives from the fact that the gauge couplings unify at energies $\sim 10^{16} \text{ GeV}$ if we adopt a supersymmetric extension of the SM in which SUSY is broken at energies $M_{SUSY} \sim \mathcal{O}(1) \text{ TeV}$ [9]. Supersymmetric particles with such large masses can be produced in the laboratory provided we have very high energies and luminosities. However their existence affects κ_V and λ_V , even at energies lower than the SUSY production threshold making them deviate from the SM predictions. Therefore the study of these quantities may furnish as a good laboratory to look for signal of supersymmetry at energies below the SUSY production threshold. In any case such studies serve as a complementary test along with other efforts towards searching for signals of new physics and supersymmetry is among the prominent candidates.

In the SM κ_V and λ_V as functions of the momentum q^2 carried by the V boson ($V = \gamma, Z$), for on shell W 's, have been studied in detail but a similar analysis has not been carried out within the context of the MSSM. Only the quantities $\kappa_\gamma(q^2 = 0)$, $\lambda_\gamma(q^2 = 0)$ have been considered which are actually related to the static quantities magnetic dipole (μ_W) and electric quadrupole (Q_W) moments of the W boson. To be of relevance for future collider experiments the form factors $\kappa_{\gamma,Z}$, $\lambda_{\gamma,Z}$ should be evaluated in the region $q^2 > 4M_W^2$. The behavior of $\kappa_{\gamma,Z}$, $\lambda_{\gamma,Z}$ in this physical region may be different from that at $q^2 = 0$ especially when the energy gets closer to M_{SUSY} and supersymmetric particles may yield sizable effects, due to the fact that we are approaching their thresholds. In those cases an enhancement of their corresponding contributions is expected, unlike SM contributions which in this high energy regime are suppressed. We should also point out that some of the supersymmetric particles may have relatively small masses, for a certain range of the parameters and in those circumstances their contributions to TGV's are not necessarily small. In order to know the magnitude of these effects a detailed computation of the trilinear gauge boson couplings should be carried out.

In this work we undertake this problem and study the C and P even $WW\gamma$, WWZ vertices in the context of the MSSM when the external W bosons are on their mass shell. Such studies are important in view of forthcoming experiments at LEP200 and other future collider experiments which will probe the structure of the gauge boson couplings and test with high accuracy the predictions of the SM. If deviations from the SM predictions are observed these experiments will signal the presence of new underlying dynamics which opens at scales larger than the Fermi scale.

The magnitude of the aforementioned couplings and their dependence on the arbitrary parameters of the MSSM requires a systematic study in which all limitations imposed by a renormalization group analysis of all running parameters involved and especially those arising from the radiative breaking of the electroweak (EW) symmetry are duly taken into account. In this paper we deal with this issue and calculate the trilinear vector boson couplings as functions of the momentum q^2 carried by the γ, Z and the arbitrary parameters of minimal supersymmetry.

This paper is organized as follows:

In section 2 we give a brief outline of the MSSM. In section 3 we carry on to discuss the SM predictions for the TGV's paying special attention to the contributions of fermions and those of the gauge bosons discussing the issue of gauge independence. In section 4 the MSSM predictions for these couplings is discussed. Section 5 deals with the absorptive (Imaginary) parts of these vertices and in section 6 we present the numerical analysis and discuss our conclusions.

2. The MSSM

The MSSM is described by a Lagrangian [10]

$$\mathcal{L} = \mathcal{L}_{SUSY} + \mathcal{L}_{soft} \quad (2)$$

where its supersymmetric part \mathcal{L}_{SUSY} is derived from a superpotential \mathcal{W} bearing the form

$$\mathcal{W} = (h_U \hat{Q}^i \hat{H}_2^j \hat{U}^c + h_D \hat{Q}^i \hat{H}_1^j \hat{D}^c + h_E \hat{L}^i \hat{H}_1^j \hat{E}^c + \mu \hat{H}_1^i \hat{H}_2^j) \epsilon_{ij} \quad , \quad \epsilon_{12} = +1 \quad (3)$$

In Eq.(3) carrets denote supermultiplets. Minimality is enforced by assuming the $SU(3) \times SU(2) \times U(1)$ as the gauge group and the least number of chiral multiplets necessary to accomodate matter fermions and drive EW symmetry breaking. The superpotential above conserves R -parity. The H_1 , H_2 Higgses give mass to up and down fermions respectively after EW breaking takes place. The part responsible for the soft breaking of supersymmetry is given by

$$\begin{aligned} -\mathcal{L}_{soft} &= \sum_i m_i^2 |\Phi_i|^2 + (h_U A_U Q H_2 U^c + h_D A_D Q H_1 D^c + h_E A_L L H_1 E^c + h.c.) \\ &+ (\mu B H_1 H_2 + h.c.) + \frac{1}{2} \sum_a M_a \bar{\lambda}_a \lambda_a. \end{aligned} \quad (4)$$

where m_i are the soft scalar masses, $A_{U,D,L}$ are trilinear soft couplings, B is the Higgs mixing parameter and M_α , $\alpha = 1, 2, 3$ are the soft gauginos masses for the $U(1)$, $SU(2)$ and $SU(3)$ gauge fermions respectively. Throughtout this paper we assume universal boundary conditions at the unification scale $M_{GUT} \simeq 10^{16} GeV$

$$m_i^2 \equiv m_0^2 \quad , \quad A_{U,D,L} \equiv A_0 \quad , \quad M_\alpha \equiv M_{1/2} \quad (5)$$

This choice is suggested by grand unification and also by absence of flavor changing neutral currents which puts stringent constraints on the difference of masses squared of the same charge squarks. However this is in no way mandatory. At least it parametrizes our ignorance concerning the origin of the soft SUSY breaking parameters in the most

economical and plausible way. We don't expect that altering the boundary conditions given in Eqs.(5) above will drastically affect the estimates for the TGV's.

The values of all running parameters in the vicinity of the electroweak scale are then given by solving their Renormalization Group Equations (RGE's) having as initial conditions Eqs. (5) ^[11].

The breaking of the EW symmetry is known to proceed via radiative corrections driven by the large top Yukawa coupling ^[11]. The equations minimizing the scalar potential of the theory are

$$\frac{M_Z^2}{2} = \frac{\bar{m}_1^2 - \bar{m}_2^2 \tan^2 \beta}{\tan^2 \beta - 1} \quad , \quad \sin 2\beta = -\frac{2B\mu}{\bar{m}_1^2 + \bar{m}_2^2} \quad (6)$$

where the angle β sets the relative strength of the v.e.v. of the H_1 and H_2 Higgs fields involved

$$\tan \beta(M_Z) \equiv \frac{v_2(M_Z)}{v_1(M_Z)}. \quad (7)$$

In Eqs. (6)–(7) all quantities are meant at M_Z , the experimental value of the Z boson mass ($M_Z = 92.18 \text{ GeV}$), and \bar{m}_1^2 , \bar{m}_2^2 are defined as

$$\bar{m}_{1,2}^2 = m_{1,2}^2 + \frac{\partial \Delta V}{\partial v_{1,2}^2} \quad , \quad m_{1,2}^2 = m_{H_{1,2}}^2 + \mu^2. \quad (8)$$

In Eq.(8) $m_{H_{1,2}}$ are the soft Higgses masses and $\bar{m}_{1,2}$ differ from $m_{1,2}$ by the contributions of the one loop corrections ΔV to the scalar potential of the theory. Including the one loop corrections within the minimizing Eqs.(6), as prescribed by Eq.(8), is a necessary ingredient for the numerical stability of our physical results. If not included the physical quantities would strongly depend on the choice of the scale at which physical quantities are evaluated leading to results that are ambiguous and untrustworthy ^[12].

The arbitrary parameters of the model are the soft parameter m_0 , A , $M_{1/2}$, B the mixing parameter μ as well as the values of the top Yukawa coupling h_t ². This number is reduced to five if use is made of the first of the minimizing equations (6). Then a convenient set of independent parameters, which is adopted by many authors, is to take the set

$$m_0 \quad , \quad A_0 \quad , \quad M_{1/2} \quad , \quad \tan \beta(M_Z) \quad , \quad m_t(M_Z) \quad (9)$$

where $m_t(M_Z)$ is the value of the “running” top quark mass at the scale M_Z . This facilitates the numerical analysis a great deal since the RGE's of all soft masses and parameters involved, with the exception of B and μ , do not depend on B , μ (nearly decouple). Given the inputs (9) the RGE's can be solved and predictions for the mass spectrum can be given. At this point we should remark that all subtleties associated with this approach, like for instance the presence of low energy thresholds and other

²The top Yukawa coupling although localized in a narrow range of values in view of the recent experimental evidence for the top quark ^[13] is being considered as an input parameter since the occurrence of symmetry breaking is very sensitive to its value.

uncertainties due to higher loop effects, in no way affect the one loop corrections to the TGV's. Complete expressions for the RGE's of all parameters involved can be traced in the literature and will not be repeated here [10, 11].

After this brief outline of the MSSM we embark to discuss the TGV's defined in the previous section.

3. The SM contribution to $\Delta k_V(Q^2)$, $\Delta Q_V(Q^2)$

Although the SM contributions to the TGV's have already been calculated in the literature [14], for reasons of completeness we shall briefly discuss them in this section too paying special attention to the contributions of fermions and gauge bosons.

In momentum space the most general WWV vertex ($V = \gamma$ or Z) with the two W 's on shell and keeping only the transvers degrees of freedom for the γ or Z can be written as [7]

$$\begin{aligned} \Gamma_{\mu\alpha\beta}^V &= -ig_{WWV} \{ f_V [2g_{\alpha\beta}\Delta_\mu + 4(g_{\alpha\mu}Q_\beta - g_{\beta\mu}Q_\alpha)] \\ &\quad + 2\Delta k_V (g_{\alpha\mu}Q_\beta - g_{\beta\mu}Q_\alpha) + 4\frac{\Delta Q_V}{M_W^2} \Delta_\mu (Q_\alpha Q_\beta - \frac{Q^2}{2}g_{\alpha\beta}) \} + \dots \end{aligned} \quad (10)$$

where $\Delta k_V \equiv k_V + \lambda_V - 1$, $\Delta Q_V \equiv -2\lambda_V$. The kinematics of the vertex is shown in Fig. 1.

The ordinary matter fermion contributions both to $Q^2 = 0$ and $Q^2 \neq 0$ have been studied elsewhere [15, 16]. However in those works there is an important sign error which affects substantially the results given in those references [17]. This has been also pointed out independently in ref. [18]. The consequences of this for the static quantities of the W boson μ_W , Q_W has been discussed in detail in ref. [17, 19]. In the massless fermion limit, which is actually the case for the first two families, this leads to nonvanishing contributions for both $\Delta k_\gamma(Q^2 = 0)$ and $\Delta Q_\gamma(Q^2 = 0)$, contrary to what had been previously claimed. These are proportional to $Tr(QT_3) \neq 0$, unlike the anomaly terms which are proportional to TrQ and hence vanishing. The details of this calculation which points out this important sign error can be traced in the literature [17]. In the SM these contributions to $\Delta k_\gamma(Q^2 = 0)$ are large and negative partially cancelling the contributions of the gauge bosons and the standard model Higgs which are positive.

In units of $g^2/16\pi^2$ the fermion contributions of the triangle graph shown in Fig. 2a are as follows,

$$\begin{aligned} \Delta k_V &= -c_V T_3^f C_g \int_0^1 dt \int_0^1 d\alpha \{ g_L^f [t^4 + t^3(-1 + R_{f'} - R_f) + t^2(R_f - R_{f'}) \\ &\quad + \frac{4Q^2}{M_W^2} t^3(3t - 2)\alpha(1 - \alpha)] + g_R^f [R_f t^2] \} \frac{1}{L_f^2} \end{aligned} \quad (11)$$

$$\Delta Q_V = -c_V T_3^f C_g g_L^f \int_0^1 dt \int_0^1 d\alpha \frac{8t^3(1 - t)(1 - \alpha)\alpha}{L_f^2} \quad (12)$$

where $c_\gamma = 1$, $c_Z = R$ with $R \equiv M_Z^2/M_W^2$. In Eqs. (11) and (12)

$$L_f^2 \equiv t^2(1 - \frac{4Q^2}{M_W^2}\alpha(1 - \alpha)) + t(R_f - R_{f'} - 1) + R_{f'} + i\epsilon \quad , \quad R_{f,f'} \equiv \frac{m_{f,f'}^2}{M_W^2}$$

and C_g is the color factor (1 for leptons, 3 for quarks). The couplings $g_{L,R}^f$ appearing in Eq.(11) are as follows

$$\begin{aligned} V = \gamma & : & g_L^f &= g_R^f = Q_{em}^f \\ V = Z & : & g_L^f &= Q_{wL}^f, \quad g_R^f = Q_{wR}^f \end{aligned}$$

where Q_{em}^f are the electromagnetic charges, and $Q_{wL,R}^f$ are the weak charges for left/right handed fermions, which are defined by the relation $Q_w^f \equiv T_3^f - Q_{em}^f \sin^2 \theta_W$. T_3^f is the weak isospin of the fermion f , ie. $T_3^f = -1/2$ for the left handed charged leptons etc. At zero momentum transfer Δk_γ , ΔQ_γ are nonvanishing as said earlier yielding $\frac{g^2}{16\pi^2}\mathcal{O}(1)$ contributions to both Δk_γ , ΔQ_γ . Actually it turns out that when $Q^2 = 0$ this is the larger contribution to ΔQ_γ of all sectors, while $\Delta k_\gamma(Q^2 = 0)$ is negative partially cancelling large ($\sim \frac{g^2}{16\pi^2}\mathcal{O}(1)$) contribution from gauge boson and Higgs particles as said previously. We should point out that Δk_V , ΔQ_V as given in Eqs.(11) and (12) refer to both the real and imaginary parts of the vertices; as we pass the internal particle threshold imaginary parts develop, too due to the $i\epsilon$ appearing in the denominator. One can easily check that as $Q^2 \rightarrow \infty$ fermion contributions to both Δk_V , ΔQ_V , tend to zero as demanded by unitarity.

Regarding the contributions of the gauge bosons to Δk_V , ΔQ_V the calculations were carried out in the 't Hooft – Feynman gauge [14], and the results are known to be gauge dependent. The details of this calculation can be traced in the literature [see Eq.(8)–(23) of ref. [14]]. In order to render the trilinear gauge boson vertices gauge independent we should add to them additional contributions from box graphs by applying special field theory techniques, such as the pinch technique [20], or work in manifestly gauge invariant gauges [21]. As a result of this gauge dependence the quantity Δk_V turns out to have bad high energy behaviour, growing logarithmically as the energy increases, violating unitarity constraints. Besides being gauge dependent Δk_V is also singular at the infrared (IR). Actually this IR singularity occurring in one of the graphs is the only one surviving among several other which cancel against each other. As said previously for the restoration of gauge independence additional contributions from some box graphs, the pinch contributions, should be appended to the vertex parts. These also cancel the IR divergence mentioned earlier. In units of $g^2/16\pi^2$ these pinch parts are given by [20],

$$\begin{aligned}\Delta\hat{k}_\gamma &= -2\frac{Q^2}{M_W^2}\{\cos^2\theta_W\int_0^1 dt\int_0^1 d\alpha\frac{t^2-2t}{t^2+R(1-t)-\frac{4Q^2}{M_W^2}t^2\alpha(1-\alpha)+i\epsilon}\\ &\quad +\sin^2\theta_W\int_0^1 dt\frac{1}{1-\frac{4Q^2}{M_W^2}t(1-t)+i\epsilon}\}+IR\end{aligned}\quad (13)$$

$$\begin{aligned}\Delta\hat{k}_Z &= -\frac{1}{2}\left(\frac{4Q^2}{M_W^2}-R\right)\{\cos^2\theta_W\int_0^1 dt\int_0^1 d\alpha\frac{t^2-2t}{t^2+R(1-t)-\frac{4Q^2}{M_W^2}t^2\alpha(1-\alpha)+i\epsilon}\\ &\quad +\sin^2\theta_W\int_0^1 dt\frac{1}{1-\frac{4Q^2}{M_W^2}t(1-t)+i\epsilon}\}+IR\quad .\end{aligned}\quad (14)$$

In Eqs. (13)–(14), $R \equiv M_Z^2/M_W^2$ while IR stands for the infrared singularities which cancel against the corresponding singularities of the vertices given in ref. [14]. Once the pinch contribution Eq.(13)–(14) are taken into account the gauge boson contributions become gauge independent approaching zero values as Q^2 increases as demanded by unitarity and are also free of infrared singularities.

4. The MSSM contribution to $\Delta k_V(Q^2)$, $\Delta Q_V(Q^2)$

At $Q^2 = 0$ the MSSM contributions to Δk_γ , ΔQ_γ have been studied elsewhere and their dependences on the soft breaking parameters A , m_0 , $M_{1/2}$, $\tan\beta$ and top quark mass m_t have been investigated [17]. The \tilde{q} , \tilde{l} (squarks, sleptons), \tilde{Z} , \tilde{C} (neutralinos, charginos) as well as the supersymmetric Higgs contributions to Δk_V , ΔQ_V are deduced from the triangle graphs shown in Figures 2 and 3. We show only graphs that yield nonvanishing contributions to at least one of the Δk_V , ΔQ_V . In the following we shall consider the contributions of each sector separately.

Squarks–Sleptons (\tilde{q} , \tilde{l})

We first consider the contributions of the sfermion sector of the theory which can be read from the diagram (b) of Figure 2. Unlike matter fermions this graph involves mixing matrices due to the fact that left \tilde{f}_L and right \tilde{f}_R handed sfermions mix when electroweak symmetry breaks down. Such mixings are substantial in the stops, due to the heaviness of the top quark, resulting to large mass splitting of the corresponding mass eigenstates $\tilde{t}_{1,2}$. For the sfermions we find after a straightforward calculation that:

$$\Delta k_V = -2C_g c_V T_3^f g_L^f \sum_{i,j=1}^2 (K_{i1}^{\tilde{f}'} K_{j1}^{\tilde{f}})^2 \int_0^1 dt \int_0^1 d\alpha \frac{t^2(1-t)(2t-1+R_{\tilde{f}_j}-R_{\tilde{f}'_i})}{L_{\tilde{f}}^2} \quad (15)$$

$$\Delta Q_V = 2C_g c_V T_3^f g_L^f \sum_{i,j=1}^2 (K_{i1}^{\tilde{f}'} K_{j1}^{\tilde{f}})^2 \int_0^1 dt \int_0^1 d\alpha \frac{4t^3(1-t)\alpha(1-\alpha)}{L_{\tilde{f}}^2} \quad (16)$$

$$L_{\tilde{f}}^2 \equiv t^2 + (R_{\tilde{f}_j} - R_{\tilde{f}'_i} - 1)t + R_{\tilde{f}'_i} - \frac{4Q^2}{M_W^2} t^2 \alpha(1-\alpha) + i\epsilon \quad , \quad R_{\tilde{f}_i, \tilde{f}'_i} \equiv (m_{\tilde{f}_i, \tilde{f}'_i}/M_W)^2$$

The prefactors appearing in the integrals above c_V, T_3^f, g_L^f and C_g , are exactly those of fermions, see Eqs. (11)–(12), since fermions and their superpartners carry same quantum numbers. $\tilde{f}_{1,2}$ and $\tilde{f}'_{1,2}$ denote the mass eigenstates while $\mathbf{K}^{\tilde{f}, \tilde{f}'}$ diagonalize the corresponding mass matrices, i.e. $\mathbf{K}^{\tilde{f}, \tilde{f}'} \mathcal{M}_{\tilde{f}, \tilde{f}'}^2 \mathbf{K}^{\tilde{f}, \tilde{f}'}{}^T = \text{diagonal}$. In the stop sector for instance, where such mixings are large, the corresponding mass matrix is given by

$$\mathcal{M}_{\tilde{t}}^2 = \begin{pmatrix} m_{Q_3}^2 + m_t^2 & m_t(A + \mu \cot \beta) \\ + M_Z^2(\cos 2\beta)(\frac{1}{2} - \frac{2}{3} \sin^2 \theta_W) & \\ m_t(A + \mu \cot \beta) & m_{U_3^c}^2 + m_t^2 \\ & + M_Z^2(\cos 2\beta)(\frac{2}{3} \sin^2 \theta_W) \end{pmatrix} \quad (17)$$

and the diagonalizing matrix is defined as $\mathbf{K}^{\tilde{t}} \mathcal{M}_{\tilde{t}}^2 \mathbf{K}^{\tilde{t}T} = \text{diagonal}(m_{\tilde{t}_1}^2, m_{\tilde{t}_2}^2)$. In the absence of SUSY breaking effects $m_{\tilde{f}, \tilde{f}'} = m_{f, f'}$ and $\mathbf{K}^{\tilde{f}, \tilde{f}'}$ become the unit matrices. In that limit ΔQ_V given above cancels against the corresponding fermionic contribution as it should.

Neutralinos–Charginos (\tilde{Z}, \tilde{C})

The neutralino and chargino sector is perhaps the most awkward sector to deal with owing to mixings originating from the electroweak symmetry breaking effects. Their contributions are read from the graphs shown in Figure 2c,d. In the following we shall denote by \tilde{C}_i the two chargino states (Dirac fermions) and by \tilde{Z}_α the four neutralino states (Majorana fermions). Recall that they are eigenstates of the following mass matrices ^[17],

$$\mathcal{M}_{\tilde{C}} = \begin{pmatrix} M_2 & -g v_2 \\ -g v_1 & \mu \end{pmatrix} \quad (18)$$

$$\mathcal{M}_{\tilde{\mathbf{N}}} = \begin{pmatrix} M_1 & 0 & g'v_1/\sqrt{2} & -g'v_2/\sqrt{2} \\ 0 & M_2 & -gv_1/\sqrt{2} & gv_2/\sqrt{2} \\ g'v_1/\sqrt{2} & -gv_1/\sqrt{2} & 0 & -\mu \\ -g'v_2/\sqrt{2} & gv_2/\sqrt{2} & -\mu & 0 \end{pmatrix} \quad (19)$$

where $v_1/\sqrt{2}$, $v_2/\sqrt{2}$ are the v.e.v.'s of the neutral components of the Higgs field H_1 and H_2 respectively. If the \mathbf{U} , \mathbf{V} matrices diagonalize $\mathcal{M}_{\tilde{\mathbf{C}}}$, i.e. $\mathbf{U}\mathcal{M}_{\tilde{\mathbf{C}}}\mathbf{V}^\dagger = \text{diagonal}$, and \mathbf{O} (real orthogonal) diagonalizes the real symmetric neutralino mass matrix of Eq.(19), $\mathbf{O}^T\mathcal{M}_{\tilde{\mathbf{N}}}\mathbf{O} = \text{diagonal}$, then the electromagnetic and weak currents are given by

$$J_{em}^\mu = \sum_i \tilde{C}_i \gamma^\mu \tilde{C}_i \quad (20)$$

$$J_+^\mu = \sum_{\alpha,i} \tilde{Z}_\alpha \gamma^\mu (P_R C_{\alpha i}^R + P_L C_{\alpha i}^L) \tilde{C}_i \quad (21)$$

$$J_0^\mu = \sum_{i,j} \tilde{C}_i \gamma^\mu (P_R A_{ij}^R + P_L A_{ij}^L) \tilde{C}_j + \frac{1}{2} \sum_{\alpha,\beta} \tilde{Z}_\alpha \gamma^\mu (P_R B_{\alpha\beta}^R + P_L B_{\alpha\beta}^L) \tilde{Z}_\beta \quad (22)$$

where

$$C_{\alpha i}^R = -\frac{1}{\sqrt{2}} O_{3\alpha} U_{i2}^* - O_{2\alpha} U_{i1}^* \quad , \quad C_{\alpha i}^L = +\frac{1}{\sqrt{2}} O_{4\alpha} V_{i2}^* - O_{2\alpha} V_{i1}^* \quad (23)$$

$$A_{ij}^h = [\cos^2 \theta_W \delta_{ij} - \frac{1}{2} (V_{i2} V_{j2}^* \delta_{hL} + U_{i2}^* U_{j2} \delta_{hR})] \quad , \quad h = L, R \quad (24)$$

$$B_{\alpha\beta}^L = \frac{1}{2} (O_{3\alpha} O_{3\beta} - O_{4\alpha} O_{4\beta}) \quad , \quad B_{\alpha\beta}^R = -B_{\alpha\beta}^L \quad (25)$$

$P_{R,L}$ are the right/left handed projection operator $(1 \pm \gamma_5)/2$. The contributions of this sector to Δk_γ , ΔQ_γ , as calculated from the graph shown in Figure 2c, is as follows:

$$\begin{aligned} \Delta k_\gamma = & - \sum_{i,\alpha} \int_0^1 dt \int_0^1 d\alpha \{ F_{\alpha i} [t^4 + (R_\alpha - R_i - 1)t^3 + (2R_i - R_\alpha)t^2 \\ & + \frac{4Q^2}{M_W^2} t^3 (3t - 2)\alpha(1 - \alpha)] + G_{\alpha i} \frac{m_i m_\alpha}{M_W^2} (4t^2 - 2t) \} \frac{1}{L_Z^2} \end{aligned} \quad (26)$$

$$\Delta Q_\gamma = -8 \sum_{i,\alpha} F_{\alpha i} \int_0^1 dt \int_0^1 d\alpha \frac{t^3 (1 - t)\alpha(1 - \alpha)}{L_Z^2} \quad (27)$$

$$L_Z^2 = t^2 + (R_i - R_\alpha - 1)t + R_\alpha - \frac{4Q^2}{M_W^2} t^2 \alpha(1 - \alpha) + i\epsilon \quad (28)$$

$$\begin{aligned} F_{\alpha i} = & |C_{\alpha i}^R|^2 + |C_{\alpha i}^L|^2 \quad , \quad G_{\alpha i} = (C_{\alpha i}^L C_{\alpha i}^{R*} + h.c.) \\ R_{\alpha,i} \equiv & \frac{m_{\alpha,i}^2}{M_W^2} \end{aligned} \quad (29)$$

where the index $\alpha = 1, 2, 3, 4$ is the neutralino index and $i = 1, 2$ is the chargino index. Note that we have not committed ourselves to a particular sign convention for the masses

m_i, m_α appearing to the sum in the equation above for the Δk_γ . Chiral rotations that makes these masses positive it also affects the rotation matrices and should be taken into account.

For the couplings $\Delta k_Z, \Delta Q_Z$ we get,
Graph of Figure 2c :

$$\begin{aligned}\Delta k_Z &= -R \sum_{i,j,\alpha} \int_0^1 dt \int_0^1 d\alpha \{ S_{ij\alpha}^L [t^2(1-t)(-t + R_i\alpha + R_j(1-\alpha) - R_\alpha) \\ &\quad + \frac{4Q^2}{M_W^2} t^3(3t-2)\alpha(1-\alpha)] + \frac{m_i m_j}{M_W^2} S_{ij\alpha}^R t^2 \\ &\quad - \frac{m_i m_\alpha}{M_W^2} (T_{ij\alpha}^L + T_{ij\alpha}^R) [2t^2\alpha + t^2 - t] \} \frac{1}{L_{ij\alpha}^2}\end{aligned}\quad (30)$$

$$\Delta Q_Z = -8R \sum_{i,j,\alpha} S_{ij\alpha}^L \int_0^1 dt \int_0^1 d\alpha \frac{t^3(1-t)\alpha(1-\alpha)}{L_{ij\alpha}^2} \quad (31)$$

where

$$\begin{aligned}S_{ij\alpha}^{L(R)} &\equiv (C_{\alpha i}^{L*} C_{\alpha j}^L A_{ji}^{L(R)} + (L \rightleftharpoons R)) \quad , \quad T_{ij\alpha}^{L(R)} \equiv (C_{\alpha i}^{L*} C_{\alpha j}^R A_{ji}^{L(R)} + (L \rightleftharpoons R)) \\ L_{ij\alpha}^2 &= \alpha t R_i + t(1-\alpha) R_j + R_\alpha(1-t) - t(1-t) - \frac{4Q^2}{M_W^2} t^2 \alpha(1-\alpha) + i\epsilon \\ R_{i,j,\alpha} &\equiv \frac{m_{i,j,\alpha}^2}{M_W^2} \quad , \quad i, j = \text{chargino indices} \quad , \quad \alpha = \text{neutralino index}\end{aligned}$$

Graph of Figure 2d :

Same as in previous graph with $\{i, j, \alpha\}$ replaced by $\{\rho, \sigma, i\}$ and $S_{ij\rho}^{L(R)}, T_{ij\rho}^{L(R)}, L_{ij\rho}^2$ replaced by the following expressions:

$$\begin{aligned}S_{\rho\sigma i}^{L(R)} &\equiv -(C_{\rho i}^{L*} C_{\sigma i}^L B_{\rho\sigma}^{L(R)} + (L \rightleftharpoons R)) \\ T_{\rho\sigma i}^{L(R)} &\equiv -(C_{\rho i}^{R*} C_{\sigma i}^L B_{\rho\sigma}^{L(R)} + (L \rightleftharpoons R)) \\ L_{\rho\sigma i}^{L(R)} &= \alpha t R_\rho + t(1-\alpha) R_\sigma + R_i(1-t) - t(1-t) - \frac{4Q^2}{M_W^2} t^2 \alpha(1-\alpha) + i\epsilon \\ \sigma, \rho &= \text{neutralino indices} \quad , \quad i = \text{chargino index}\end{aligned}$$

Higgses (H_0, h_0, A, H_\pm)

There are five physical Higgs bosons which survive electroweak symmetry breaking. Two of these, H_0 and h_0 , are neutral and CP even, while a third A , is neutral and CP

odd. The remaining Higgses bosons, H_{\pm} , are charged. At the tree level the lightest of these, namely h_0 , is lighter than the Z gauge boson itself. However it is well known that radiative corrections which are due to the heavy top are quite large and should be taken into account. These modify its tree level mass by large amounts $\delta m_{h_0}^2 \sim g^2(m_t^4/M_W^2) \ln(m_{t_1}^2 m_{t_2}^2/m_t^4)$ which may push its mass up to values exceeding M_Z ; in some cases up to $\simeq 130 \text{ GeV}$. h_0 turns out to yield the largest contributions of all Higgses to the TGV's since the remaining Higgses have large masses of the order of the SUSY breaking scale. At the tree level the masses of all Higgs bosons involved are given by the following expressions :

$$m_A^2 = -\frac{2m_3^2}{\sin 2\beta} \quad , \quad (m_3^2 \equiv B\mu) \quad (32)$$

$$m_{H_0, h_0}^2 = \frac{1}{2} \{ (m_A^2 + M_Z^2)^2 \pm \sqrt{(m_A^2 + M_Z^2)^2 - 4M_Z^2 m_A^2 \cos^2(2\beta)} \} \quad (33)$$

$$m_{H_{\pm}}^2 = m_A^2 + M_W^2 \quad (34)$$

The Higgs contributions can be expressed in terms of their masses and an angle θ , which relates the states $S_1 \equiv \cos \beta (\text{Real } H_1^0) + \sin \beta (\text{Real } H_2^0)$, $S_2 \equiv -\sin \beta (\text{Real } H_1^0) + \cos \beta (\text{Real } H_2^0)$ to the mass eigenstates h_0, H_0 . The state S_1 is the SM Higgs boson which however is not a mass eigenstate since it mixes with S_2 . When $\sin^2 \theta = 1$ such a mixing does not occur and h_0 becomes the standard model Higgs bosons S_1 .

The contributions of the Higgs bosons to Δk_γ , ΔQ_γ , follow from the graphs shown in Figure 3 and are as follows,

Graphs of Figures 3a and 3b :

$$A : \quad \Delta k_\gamma = D_2(R_A, R_+) \quad , \quad \Delta Q_\gamma = Q(R_A, R_+) \quad (35)$$

$$h_0 : \quad \Delta k_\gamma = \sin^2 \theta D_1(R_{h_0}) + \cos^2 \theta D_2(R_{h_0}, R_+) \quad (36)$$

$$\Delta Q_\gamma = \sin^2 \theta Q(R_{h_0}, 1) + \cos^2 \theta Q(R_{h_0}, R_+) \quad (37)$$

$$H_0 : \quad \text{As in } h_0 \text{ with } R_{h_0} \rightarrow R_{H_0} \text{ and } \sin^2 \theta \rightleftharpoons \cos^2 \theta \quad (38)$$

$$R_a \equiv (m_a/M_W)^2 \quad , \quad a = h_0, H_0, A, H_{\pm} \quad , \quad \sin^2 \theta = \frac{M_A^2 + M_Z^2 \sin^2 2\beta - M_{h_0}^2}{M_{H_0}^2 - M_{h_0}^2} \quad .$$

The functions $D_{1,2}, Q$ appearing above are defined in Appendix A.

For the Δk_Z , ΔQ_Z form factors there are more graph contributing. These are shown in Figures 3c–3f. From the graphs shown in Figure 3 we pick the following contributions, Graph of Figure 3a:

$$\begin{aligned} \Delta k_Z = & \frac{1}{4} \{ (\cos^2 \theta) \int_0^1 dt \int_0^1 d\alpha [(4 - 2R)t^4 + (R - 2)(R_{H_0} + 2)t^3 \\ & + (2R_{H_0} - RR_{H_0} + 8 - 2R)t^2] \frac{1}{L_{H_0}^2} + (\sin^2 \theta) \times (H_0 \rightarrow h_0) \} \end{aligned} \quad (39)$$

$$\begin{aligned}
\Delta Q_Z &= (2 - R) \{ (\cos^2 \theta) \int_0^1 dt \int_0^1 d\alpha \frac{t^3(1-t)\alpha(1-\alpha)}{L_{H_0}^2} \\
&\quad + (\sin^2 \theta) \times (H_0 \rightarrow h_0) \} \\
L_{H_0}^2 &\equiv t^2 + R_{H_0}(1-t) - \frac{4Q^2}{M_W^2} t^2 \alpha(1-\alpha) + i\epsilon \quad , \quad R_{H_0, h_0} \equiv \frac{m_{H_0, h_0}^2}{M_W^2}
\end{aligned} \tag{40}$$

Graph of Figure 3b :

$$\Delta k_Z = \left(\frac{2-R}{2}\right) \{ D_2(R_A, R_+) + \sin^2 \theta D_2(R_{H_0}, R_+) + \cos^2 \theta D_2(R_{h_0}, R_+) \} \tag{41}$$

$$\Delta Q_Z = \left(\frac{2-R}{2}\right) \{ Q(R_A, R_+) + \sin^2 \theta Q(R_{H_0}, R_+) + \cos^2 \theta Q(R_{h_0}, R_+) \} \tag{42}$$

Graphs of Figures 3c and 3d :

$$\begin{aligned}
\Delta k_Z &= \frac{R}{2} \{ (\sin^2 \theta) \int_0^1 dt \int_0^1 d\alpha \frac{t^2(1-t)(1+R_+ - R_A\alpha - R_{H_0}(1-\alpha) - 2t)}{\tilde{L}_{H_0}^2} \\
&\quad + (\cos^2 \theta) \times (H_0 \rightarrow h_0) \}
\end{aligned} \tag{43}$$

$$\Delta Q_Z = 2R \{ (\sin^2 \theta) \int_0^1 dt \int_0^1 d\alpha \frac{\alpha(1-\alpha)t^3(1-t)}{\tilde{L}_{H_0}^2} + (\cos^2 \theta) \times (H_0 \rightarrow h_0) \} \tag{44}$$

$$\tilde{L}_{H_0}^2 \equiv -t(1-t) + R_A\alpha t + R_{H_0}(1-\alpha)t + R_+(1-t) - \frac{4Q^2}{M_W^2} t^2 \alpha(1-\alpha) + i\epsilon \tag{45}$$

and finally,

Graphs of Figures 3e and 3f :

$$\begin{aligned}
\Delta k_Z &= \frac{R}{2} \{ (\cos^2 \theta) \int_0^1 dt \int_0^1 d\alpha [-6\alpha t^2 + (t^3 - t^2)(2(t-1) + (R - R_{H_0})\alpha + R_{H_0}) \\
&\quad + 2(R-1)\alpha t^2] \frac{1}{\hat{L}_{H_0}^2} + (\sin^2 \theta) \times (H_0 \rightarrow h_0) \}
\end{aligned} \tag{46}$$

$$\Delta Q_Z = 2R \{ (\cos^2 \theta) \int_0^1 dt \int_0^1 d\alpha \frac{\alpha(1-\alpha)t^3(1-t)}{\hat{L}_{H_0}^2} \} + (\sin^2 \theta) \times (H_0 \rightarrow h_0) \tag{47}$$

$$\hat{L}_{H_0}^2 \equiv (1-t)^2 + R\alpha t + R_{H_0}t(1-\alpha) - \frac{4Q^2}{M_W^2} t^2 \alpha(1-\alpha) + i\epsilon \tag{48}$$

In the most of the parameter space the Higgses A, H_\pm and H_0 turn out to be rather heavy having masses of the order of the SUSY breaking scale; therefore all graphs in which at least one of these participates are small. At the same time $\sin^2 \theta$ has a value very close to unity. Thus the dominant Higgs contribution arises solely from the graphs of Figures 3a,e and 3d in which a h_0 is exchanged. This is exactly what one gets in the SM with h_0 playing the role of the SM Higgs boson.

5. The Absorptive Parts of the TGV's

The contributions of the TGV's presented so far have also imaginary (absorptive) parts which show up as soon as one passes the thresholds associated with the particles exchanged in the one loops graphs. Since the majority of the one loop expressions encountered have a triangle structure some of these thresholds can be anomalous and this depends on the masses of the particles circulating in the loop.

The absorptive parts can be readily calculated using the $i\epsilon$ prescription. Actually the denominators of the Feynman integrals involved carry a small positive imaginary part and it is a matter of a proper algebraic manipulation to pick up the relevant imaginary parts of all integral expressions presented in the previous sections. All graphs yielding nonvanishing contributions to $\Delta k_{\gamma,Z}$, $\Delta Q_{\gamma,Z}$ have a triangular structure with the exception of some of the gauge boson graphs which involve the quartic gauge boson coupling. For these we have $\Delta Q_{\gamma,Z} = 0$ with $\Delta k_{\gamma,Z}$ given by ^[14]

$$\begin{aligned}\Delta k_{\gamma,Z} &= \frac{21}{2}\sin^2\theta_W - \frac{3}{2R}\int_0^1 dt \frac{2t^3 - (8+R)t^2 + 4Rt}{t^2 + R(1-t) + i\epsilon} \\ &+ \frac{9}{2}\int_0^1 dt \ln\left(1 - \frac{4Q^2}{M_W^2}t^2\alpha(1-\alpha) + i\epsilon\right)\end{aligned}\quad (49)$$

where ($R \equiv M_Z^2/M_W^2$). The first of the integrals in the expression above does not have any discontinuity since the denominator never vanishes ³ The second integral developes an absorptive part when the argument of the logarithm becomes negative. Therefore it has an Imaginary part given by

$$Im \Delta k_{\gamma,Z} = \frac{9\pi}{2}\Theta(Q^2 - M_W^2)\sqrt{\left(1 - \frac{M_W^2}{Q^2}\right)}\quad (50)$$

For the pinch contributions we have an absorptive part arising from the single dt integrations appearing in the Eqs. (13),(14) and an additional contribution which stems from the double $dt, d\alpha$ integrations of these equations. The later yield absorptive parts, denoted by $\Delta_{\gamma,Z}$, which have a structure akin to those of the triangle graphs. The former yield absorptive parts which are easily calculated leading to the following results:

$$Im \hat{\Delta} k_{\gamma} = \pi \sin^2\theta_W \frac{\Theta(Q^2 - M_W^2)}{\sqrt{\left(1 - \frac{M_W^2}{Q^2}\right)}} + \Delta_{\gamma}\quad (51)$$

$$Im \hat{\Delta} k_Z = \pi \sin^2\theta_W \left(1 - R \frac{M_W^2}{4Q^2}\right) \frac{\Theta(Q^2 - M_W^2)}{\sqrt{\left(1 - \frac{M_W^2}{Q^2}\right)}} + \Delta_Z\quad (52)$$

³ Actually this integral arises from a diagram that has the structure of a two point Greens function. It involves the quartic gauge coupling where one of its legs is the γ or Z and the other is one of the on shell external W 's. Since the W 's are on their mass shell it does not depend on Q^2 .

The absorptive parts of all triangle graphs as well as the contributions $\Delta_{\gamma,Z}$ in the Equations (51) and (52) above can be inferred by calculating the imaginary part of the integral

$$I \equiv \int_0^1 dt \int_0^1 d\alpha \frac{P_2 \alpha^2 + P_1 \alpha + P_1}{\rho + \sigma \alpha + \frac{4Q^2}{M_W^2} t^2 \alpha (1 - \alpha) + i\epsilon} \quad (53)$$

where $P_{0,1,2}$ as well as ρ, σ are functions of the variable t alone. The absorptive part of this integral is not difficult to calculate, and the details are presented in the Appendix B. In its final form it can be expressed as an single integral over the variable t (see Eq. (58), Appendix B) which can be integrated numerically using special numerical routines. Having expressed the Imaginary parts of all contributions involved, as integrals in t of known functions of t and the energy variable Q^2 , we are ready to proceed to numerical computations.

The strategy we follow for the evaluation of the absorptive parts will also apply to the real (dispersive) parts of the form factors under consideration. In fact whenever a double $\int_0^1 dt \int_0^1 d\alpha$ integrations are encountered we first perform the $\int_0^1 d\alpha$ integrations explicitly and subsequently evaluate the $\int_0^1 dt$ integrations numerically for various values of Q^2 and the MSSM parameters. The details of the numerical analysis is the subject of the following section.

6. Numerical Analysis – Conclusions

As discussed in the previous section both dispersive and absorptive parts of the trilinear $WW\gamma$, WWZ vertices can be cast as single integrals of known functions of t and Q^2 , which also depend on the physical masses of all particles involved. These integrations we have numerically carried out using special routines of the FORTRAN Library *IMSL* available to us. The advantage of using this facility is that it leads to reliable results even in cases where the integrands exhibit fast growth at some points or have a rapid oscillatory behaviour. The inputs in these calculations are the value of the energy variable Q^2 and the arbitrary parameters of the MSSM discussed in the section 2.

In our numerical analysis we have taken all Yukawa couplings, but that of the top quark vanishing, which is a very good approximation especially for the reason that the trilinear gauge boson vertices under consideration are already of one loop order. This approximation however holds provided the value of the parameter $\tan\beta(M_Z)$ which sets the relative strength of the v.e.v's of the two Higgses involved are not large ≤ 10 . For larger values the bottom Yukawa coupling should be also considered in the RGE's of all running parameters involved. However this approximation little affects our numerical results for the form factors under consideration.

With the experimental inputs $M_Z = 91.18 \text{ GeV}$, $\sin^2 \theta_W = .239$, $\alpha_{em}(M_Z) = 1/129$ and $\alpha_s(M_Z) = .117$ and with given values for the arbitrary parameters $\tan\beta(M_Z)$,

$m_t(M_Z)$, A_0 , m_0 , $M_{1/2}$ we run our numerical routines in order to know the mass spectrum and the relevant mixing parameters necessary for the evaluation of the form factors given in the previous sections. Throughout the analysis we have taken ⁴ $\tan\beta(M_Z) \leq 10$, but its value cannot be taken arbitrarily small. Actually given $m_t(M_Z)$ the parameter $\tan\beta(M_Z)$ is forced to a minimum value otherwise Landau poles are encountered making the top Yukawa coupling $h_t^2/(4\pi)^2$ getting values ≥ 1 outside the validity of the perturbative regime.

For the running top quark mass $m_t(M_Z)$ we took values in the whole range from 130 GeV to 190 GeV , although small values of m_t are already ruled out experimentally in view of the recent *CDF* and *D0* results which both quote a mass for the top quark larger than about 170 GeV [13]. The physical top quark masses emerging out are slightly larger by about 3% ⁵.

As for the soft SUSY breaking parameters A_0 , m_0 , $M_{1/2}$ we scan the three dimensional parameter space from $\simeq 100\text{ GeV}$ to 1 TeV . This parameter space can be divided into three main regions:

- i) $A_0 \simeq m_0 \simeq M_{1/2}$ (all SUSY breaking terms comparable)
- ii) $A_0 \simeq m_0 \ll M_{1/2}$ (the gaugino mass is the dominant source of SUSY breaking)
- iii) $M_{1/2} \ll A_0 \simeq m_0$ (A_0, m_0 dominate over $M_{1/2}$)

Case ii) covers the no-scale models for which in most of the cases the preferable values are $A_0 = m_0 = 0$ while case iii) the light gluino case.

Regarding the values scanned for the energy variable Q^2 we moved both in the timelike and spacelike region for values ranging from $|Q^2| = 0$ to $\sqrt{|Q^2|} = 10^5 M_W$. For the timelike case, which is of relevance for future collider experiments, this corresponds to values of \sqrt{s} ranging from 0 GeV to about $600 M_W$. For comparison we quote that \sqrt{s} at LEP200 will be 190 GeV that is it just exceeds the two W 's production threshold energy $2M_W$. Both in the spacelike and timelike energy region as soon as \sqrt{s} exceeds $\simeq \text{few TeV}$ the contributions of each sector separately becomes negligible approaching zero as the energy increases in accord with unitarity requirements.

Sample results are presented in Tables I and II for values of $(A_0, m_0, M_{1/2})$ equal to $(300, 300, 300)$, $(0, 0, 300)$ and $(300, 300, 80)\text{ GeV}$ representative of the cases i), ii) and iii) respectively discussed above. The inputs for the remaining parameters are $\tan\beta(M_Z) = 2$, $m_t(M_Z) = 170\text{ GeV}$. The value of \sqrt{s} in these tables are respectively 190 and 500 GeV , corresponding to the center of mass energy of LEP200 and NLC. In the same tables for comparison we give the SM predictions for Standard Model Higgs masses $50, 100$ and 300 GeV . With the inputs given above the typical SUSY breaking scale lies in somewhere between $2M_W$ and $.5\text{ TeV}$. Although many sparticle thresholds exist in this region, as for instance the lightest of the sleptons and squarks as well as the lightest of the neutralinos and charginos, especially when $M_{1/2}$ is light, these thresholds do not

⁴ Our results for Δk_V , ΔQ_V are not sensitive to the choice of the angle β .

⁵ The physical top quark mass M_t in the DR scheme is given by $M_t = m_t(M_t)/(1 + 5\alpha_3(M_t)/3\pi)$.

result in any enhancement of the form factors $\Delta k_{\gamma,Z}$, $\Delta Q_{\gamma,Z}$. Increasing the value of the dominant SUSY breaking scale the supersymmetric contributions to these quantities become less important approaching zero values. Of all sectors the sfermions yield the smaller contributions in the entire parameter space even in cases where due to large electroweak mixings some of the squarks, namely one of the stops, are relatively light. The supersymmetric Higgses yield contributions comparable to those of the SM, provided the latter involves a light Higgs with mass around the 100 GeV scale. The bulk of the Higgs contributions is due to the lightest CP even neutral h_0 . As discussed in previous sections the dominant Higgs contributions come from the diagrams of Figures 3a,e and 3f in which a light Higgs h_0 is exchanged. These are actually the only sources of Higgs contributions in the SM with h_0 replaced by the Standard Model Higgs boson.

The last sector to be discussed is the neutralinos and charginos which in some cases, depending on the given inputs, can accomodate light states. Their contributions in that case are not necessarily small and is the principal source of deviations from the SM predictions. The contributions of the neutralinos and charginos are sensitive to the input value for the soft gaugino mass $M_{1/2}$ being more important for values $M_{1/2} < 100\text{ GeV}$. For such values of the soft gaugino mass and in the unphysical region, $0 < \sqrt{s} < 2M_W$ they are enhanced, due to the development of an anomalous threshold in this region, which results to sizable corrections to the magnetic dipole and electric quadrupole moments of the W boson [17, 19].

In Figure 4 and 5 we plot the contributions of the Higgses and of the neutralino - chargino sector to $\Delta k_{\gamma,Z}$, $\Delta Q_{\gamma,Z}$ for the most physically interesting case (300, 300, 80) GeV and for values of \sqrt{s} ranging from 0 GeV to 1 TeV . The region from 0 to $2M_W$ is unphysical since the external W 's have been taken on their mass shell. At $s = 0$ the quantities Δk_γ , ΔQ_γ are linearly related to the magnetic moment and electric quadrupole moments of the W -boson.

The structure shown in the Higgs contributions for $\sqrt{s} \leq 200\text{ GeV}$ is due to the lightest of the Higgses. One observes a fast fall off as we increase the energy to values above $\approx 200\text{ GeV}$. In the neutralino and chargino sector, and for the $\mu > 0$ case, a sharp peak is observed in the unphysical region, $\sqrt{s} < 2M_W$ due to the appearance of the anomalous threshold discussed previously and the contributions of this sector is substantially enhanced. However such an enhancement does not occur in the physical region since their contributions fall rapidly to zero as we depart from the unphysical region to values of energies above the two W production threshold. This behaviour is clearly seen in Figure 5. The structure observed at energies around 700 GeV comes from the graph of Figure (3d) and is due to the fact that for these energies we are close to thresholds associated with the heavy neutralino states.

The total contributions to the TGV's both in the MSSM and SM are shown in Figures 6 to 8. We display both dispersive and absorptive parts of the form factors under consideration. One notices that all form factors tend to zero fairly soon with increasing the energy reaching their asymptotic values at energies $\sqrt{s} \approx \text{few TeV}$ in agreement with unitarity constraints.

Our conclusion is that for energies $2M_W < \sqrt{s} < 200\text{ GeV}$ the MSSM predictions

differ in general from those of the SM but they are of the same order of magnitude. Deviations from the SM predictions to be detectable require sensitivities reaching the per mille level and hence unlikely to be observed at LEP200. If deviations from the SM predictions are observed at these energies will be the signal of new underlying dynamics which however will not be of supersymmetric nature. At higher energies SM and MSSM predictions fall rapidly to zero, due to unitarity, getting smaller by almost an order of magnitude already at energies $\sqrt{s} \approx .5 \text{ TeV}$. As a result, the task of observing deviations from the SM which are due to supersymmetry becomes even harder at these energies demanding higher experimental accuracies.

Acknowledgements

Work supported by EEC Human Capital and Mobility Program, CHRX – CT93 - 0319.

A Appendix

The functions $D_1(r)$, $D_2(r, R)$ and $Q(r)$ through which the Higgs contributions are expressed are defined as follows:

$$D_1(r) \equiv \frac{1}{2} \int_0^1 dt \int_0^1 d\alpha \frac{2t^4 + (-2-r)t^3 + (4+r)t^2}{t^2 + r(1-t) - \frac{4Q^2}{M_W^2} t^2 \alpha(1-\alpha) + i\epsilon} \quad (54)$$

$$D_2(r, R) \equiv \frac{1}{2} \int_0^1 dt \int_0^1 d\alpha \frac{2t^4 + (-3-r+R)t^3 + (1+r-R)t^2}{t^2 + (-1-r+R)t + r - \frac{4Q^2}{M_W^2} t^2 \alpha(1-\alpha) + i\epsilon} \quad (55)$$

$$Q(r, R) \equiv 2 \int_0^1 dt \int_0^1 d\alpha \frac{t^3(1-t)\alpha(1-\alpha)}{t^2 + (-1-r+R)t + r - \frac{4Q^2}{M_W^2} t^2 \alpha(1-\alpha) + i\epsilon} \quad (56)$$

B Appendix

The Imaginary part of the integral I defined in the main text (see Eq. 53) is given by

$$Im I = -\pi \int_0^1 dt \int_0^1 d\alpha (P_2 \alpha^2 + P_1 \alpha + P_0) \times \delta \left(\frac{4Q^2}{M_W^2} t^2 \alpha(1-\alpha) + \sigma \alpha + \rho \right) \quad (57)$$

The roots $\rho_{1,2}$ of the argument of the delta function in the expression above are given by

$$\lambda_{1,2} = \frac{1}{2} \left[\left(1 - \frac{\sigma}{\hat{s}t^2}\right) \pm \sqrt{\left(1 - \frac{\sigma}{\hat{s}t^2}\right)^2 - 4 \frac{\rho}{\hat{s}t^2}} \right] \quad , \quad \hat{s} \equiv \frac{4Q^2}{M_W^2}$$

The imaginary part $Im I$ vanishes if

$$\left(1 - \frac{\sigma}{\hat{s}t^2}\right)^2 - 4 \frac{\rho}{\hat{s}t^2} < 0.$$

After a straightforward calculation one arrives at the following result

$$Im I = -\pi \sum_{i=1,2} \int_0^1 dt (P_2 \lambda_i^2 + P_1 \lambda_i + P_0) \Theta(\lambda_i) \Theta(1 - \lambda_i) \times \frac{\Theta((\hat{s}t^2 - \sigma)^2 - 4 \rho t^2 \hat{s})}{\sqrt{(\hat{s}t^2 - \sigma)^2 - 4 \rho t^2 \hat{s}}} \quad (58)$$

References

- [1] W. Hollik, in “*Lepton and Photon Interactions*”, Proceedings of the XVI International Symposium, Ithaca, New York, 1993, ed. by P. Drell and D. Rubin, AIP Conf. Proc. No. 302 (AIP, New York, 1994);
D. Scaile, in *Proceedings of the International Symposium on Vector Boson self Interactions*, UCLA, Los Angeles, February 1-3 1995 (to appear).
- [2] M. Schwarz, in “*Lepton and Photon Interactions*” [1].
- [3] M. Davier and D. Treille, in *Proceedings of the ECFA workshop on LEP200*, Aachen, Germany 1986, ed. by A. Böhm and W. Hoogland (CERN Report No 87-08, Geneva, Switzerland).
- [4] M. Bilenky, J. L. Kneur, F. M. Renard and D. Schildknecht, Nucl. Phys. B409 (1993) 22; BI-TP 93/43, PM 93/14 (preprint);
G. L. Kane, J. Vidal and C. P. Yuan, Phys. Rev. D39 (1989) 2617;
J. Busenitz, in *Proceedings of the International Symposium on Vector Boson self Interactions* [1].
- [5] UA2 collaboration, Phys. Lett. B227 (1992) 191;
CDF and D0 collaborations, S. Errede in *Proceedings of the 27th International Conference on High Energy Physics*, Glasgow, Scotland, July 20-27, 1994.
- [6] J. Fleitcher, J. L. Kneur, K. Kolodziej, M. Kuroda and D. Schildknecht, Nucl. Phys. B378 (1992) 443;
D. Zeppenfeld, in *Proceedings of the International Symposium on Vector Boson self Interactions* [1];
S. Godfrey, *ibid.* ;
J. Womersky, *ibid.* ;
T. Barklow, *ibid.*
- [7] K. F. Gaemers and G. J. Gounaris, Z. Phys. C1 (1979) 259;
K. Hagiwara, R. D. Peccei, D. Zeppenfeld and K. Hikasa, Nucl. Phys. B282 (1987) 253;
U. Baur and D. Zeppenfeld, Nucl. Phys. B308 (1988) 127; B325 (1989) 253;
D. Zeppenfeld, Phys. Lett. B183 (1987) 380.
- [8] D. Zeppenfeld and S. Willenbrock, Phys. Rev. D37 (1988) 1775;
A. F. Falk, M. Luke and E. H. Simmons, Nucl. Phys. B365 (1991) 523;
E. N. Argyres and C. G. Papadopoulos, Phys. Lett. B263 (1991) 298;
A. de Rujula, M. B. Gavela, P. Hernandez and E. Masso, Nucl. Phys. B384 (1992) 298;
G. Gounaris and F. M. Renard, Z. Phys. C59 (1993) 143;
G. Gounaris, J. Layssac and F. M. Renard, Univ. of Montpellier PM 93/26, (preprint).

- [9] J. Ellis, S. Kelley and D. V. Nanopoulos, Phys. Lett. B260 (1991) 131;
U. Amaldi, W. De Boer and M. Fürstenau, Phys. Lett. B260 (1991) 447;
P. Langacker and M. Luo, Phys. Rev. D44 (1991) 817.
- [10] For reviews see:
H. P. Nilles, Phys. Rep. 110 (1984) 1 ;
H. E. Haber and G. L. Kane, Phys. Rep. 117 (1985) 75 ;
A. B. Lahanas and D. V. Nanopoulos, Phys. Rep. 145 (1987) 1.
- [11] L. E. Ibañez and G. G. Ross, Phys. Lett. 110 (1982) 215;
K. Inoue, A. Kakuto, H. Komatsu and S. Takeshita, Progr. Theor. Phys. 68 (1982) 927, *ibid.* 71 (1984) 96;
J. Ellis, D. V. Nanopoulos and K. Tamvakis, Phys. Lett. B121 (1983) 123;
L. E. Ibañez , Nucl. Phys. B218 (1983) 514 ;
L. Alvarez-Gaumé, J. Polchinski and M. Wise, Nucl. Phys. B221 (1983) 495;
J. Ellis, J. S. Hagelin, D.V. Nanopoulos and K. Tamvakis, Phys. Lett. B125 (1983) 275;
L. Alvarez-Gaumé, M. Claudson and M. Wise, Nucl. Phys. B207 (1982) 96;
C. Kounnas, A. B. Lahanas, D. V. Nanopoulos and M. Quiros, Phys. Lett. B132 (1983) 95, Nucl. Phys. B236 (1984) 438;
L. E. Ibañez and C. E. Lopez, Phys. Lett. B126 (1983) 54, Nucl. Phys. B233 (1984) 511;
G. G. Ross and R. G. Roberts, Nucl. Phys. B377 (1992) 571.
- [12] G. Gamberini, G. Ridolfi and F. Zwirner, Nucl. Phys. B331 (1990) 331;
R. Arnowitt and P. Nath, Phys. Rev. D46 (1992) 3981;
D. J. Castaño, E. J. Piard and P. Ramond, Phys. Rev. D49 (1994) 4882.
- [13] F. Abe et. al, CDF collaboration, Phys. Rev. Lett. 74 (1995) 2626;
S. Abachi et. al, D0 collaboration, Phys. Rev. Lett. 74 (1995) 2632.
- [14] E. N. Argyres, G. Katsilieris, A. B. Lahanas, C. G. Papadopoulos and V. C. Spanos, Nucl. Phys. B391 (1993) 23.
- [15] W. A. Bardeen, R. Gastmans and B. Lautrup, Nucl. Phys. B46 (1972) 319.
- [16] G. Couture and J. N. Ng, Z. Phys. C35 (1987) 65.
- [17] A. B. Lahanas and V. C. Spanos, Phys. Lett. B334 (1994) 378.
- [18] A. Culatti, Padova University preprint, DFPD/94/TH/25.
- [19] A. B. Lahanas, in *Proceedings of the International Symposium on Vector Boson self Interactions* [1], and references therein.

- [20] J. Papavassiliou and K. Phillipides, Phys. Rev. D48 (1993) 4255;
J. Papavassiliou, Phys. Rev. D50 (1994) 5958;
J. Papavassiliou and K. Phillipides, N.Y. University preprint, hep-ph/9503246;
J. Papavassiliou, in *Proceedings of the International Symposium on Vector Boson self Interactions* [1];
K. Phillipides, *ibid.*
- [21] A. Drenner, G. Weiglein and S. Dittmaier, Phys. Lett. B333 (1994) 420;
S. Hashimoto, J. Kodaira, Y. Yasui and K. Sasaki, Phys. Rev. D50 (1994) 7066.

Table Captions

Table I: MSSM predictions for $\Delta k_{\gamma,Z}$, $\Delta Q_{\gamma,Z}$, in units of $g^2/16\pi^2$, for three different inputs of $A_0, m_0, M_{1/2}$. Both $\mu > 0$ and $\mu < 0$ cases are displayed. The energy is $\sqrt{s} = 190 \text{ GeV}$. The SM predictions for Higgs masses 50, 100 and 300 GeV respectively are also displayed.

Table II: MSSM predictions for $\Delta k_{\gamma,Z}$, $\Delta Q_{\gamma,Z}$, in units of $g^2/16\pi^2$, for three different inputs of $A_0, m_0, M_{1/2}$. Both $\mu > 0$ and $\mu < 0$ cases are displayed. The energy is $\sqrt{s} = 500 \text{ GeV}$. The SM predictions for Higgs masses 50, 100 and 300 GeV respectively are also displayed.

Figure Captions

Figure 1: The kinematics of the WWV vertex.

Figure 2: Fermion and sfermion contributions to the WWV vertices [figs. a,b]. Neutralino (\tilde{Z}) and Chargino (\tilde{C}) contributions to $WW\gamma$ [fig. c] and WWZ [figs. c,d] vertices.

Figure 3: Higgs graphs contributing to the $WW\gamma$ and WWZ trilinear vertices. h_0 denotes the lightest neutral Higgs boson.

Figure 4: MSSM Higgs contributions to the dispersive parts of Δk_γ , ΔQ_γ (solid lines) and Δk_Z , ΔQ_Z (dashed lines), in units of $g^2/16\pi^2$, as functions of the energy \sqrt{s} . The inputs are $(A_0, m_0, M_{1/2}) = (300, 300, 80) \text{ GeV}$, $\tan \beta = 2$, $m_t = 170 \text{ GeV}$. Both $\mu > 0$ and $\mu < 0$ cases are displayed. The vertical dotted line indicates the position of the $2W$ production threshold.

Figure 5: As in Figure 4 for the Neutralino and Chargino contributions.

Figure 6: MSSM predictions for $\Delta k_{\gamma,Z}$, $\Delta Q_{\gamma,Z}$. The parameters are as in Figure 4.

Figure 7: MSSM predictions for the absorptive parts of $\Delta k_{\gamma,Z}$, $\Delta Q_{\gamma,Z}$. The parameters are as in Figure 4.

Figure 8: SM predictions for the dispersive [figs. a,b] and absorptive [figs. c,d] parts of $\Delta k_{\gamma,Z}$, $\Delta Q_{\gamma,Z}$ for a Standard Model Higgs mass equal to 100 GeV and $m_t = 170 \text{ GeV}$.

TABLE I			
$A_0, m_0, M_{1/2}$	300, 300, 80 $\tan \beta = 2$	[300, 300, 300] $m_t = 170 \text{ GeV}$	(0,0,300)
$\sqrt{s} = 190 \text{ GeV}$	$\mu > 0$		$\mu < 0$
Δk_γ	-1.938 [-1.742] (-1.762)		-1.733 [-1.767] (-1.791)
ΔQ_γ	0.906 [0.526] (0.538)		0.300 [0.529] (0.540)
Δk_Z	-2.282 [-2.155] (-2.154)		-2.016 [-2.146] (-2.140)
ΔQ_Z	-0.354 [0.345] (0.334)		-1.193 [0.363] (0.357)
<i>SM predictions</i>	$\Delta k_\gamma = -2.005, -1.735, -2.118$ $\Delta Q_\gamma = .524, .530, .503$		$\Delta k_Z = -1.350, -2.437, -1.404$ $\Delta Q_Z = .507, .533, .481$

TABLE II			
$A_0, m_0, M_{1/2}$	300, 300, 80 $\tan \beta = 2$	[300, 300, 300] $m_t = 170 \text{ GeV}$	(0,0,300)
$\sqrt{s} = 500 \text{ GeV}$	$\mu > 0$		$\mu < 0$
Δk_γ	-.262 [-.151] (-.191)		-.310 [-.207] (-.259)
ΔQ_γ	0.150 [0.030] (0.056)		0.146 [0.041] (0.069)
Δk_Z	0.121 [0.204] (0.209)		0.240 [0.191] (0.198)
ΔQ_Z	0.358 [-.407] (-.427)		0.256 [-.325] (-.352)
<i>SM predictions</i>	$\Delta k_\gamma = -.250, -.168, .046$ $\Delta Q_\gamma = .054, .057, .064$		$\Delta k_Z = .147, .208, -.036$ $\Delta Q_Z = .057, .058, .077$

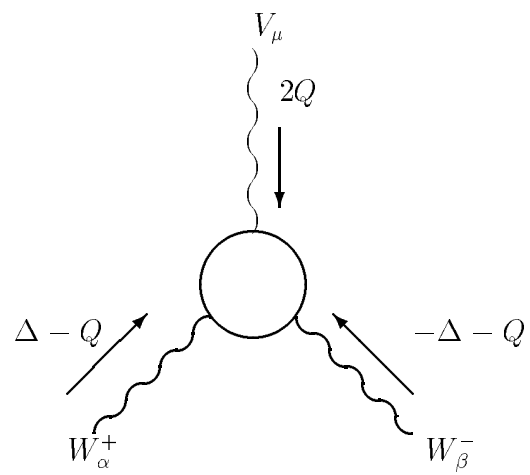


Figure 1

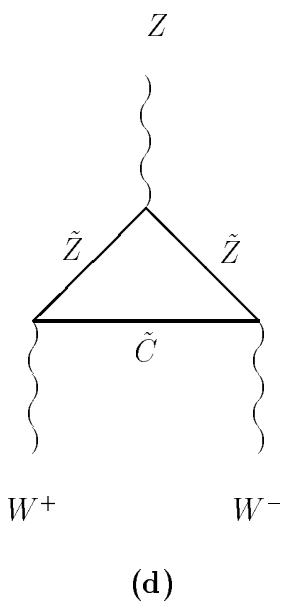
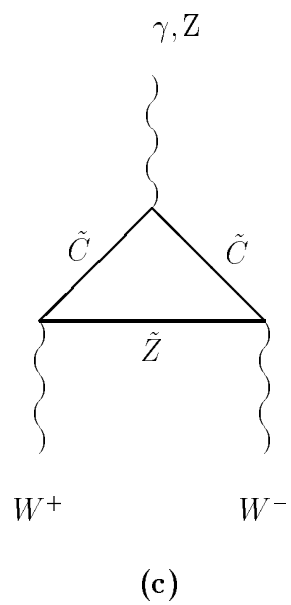
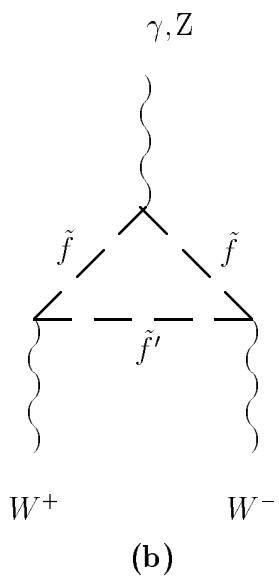
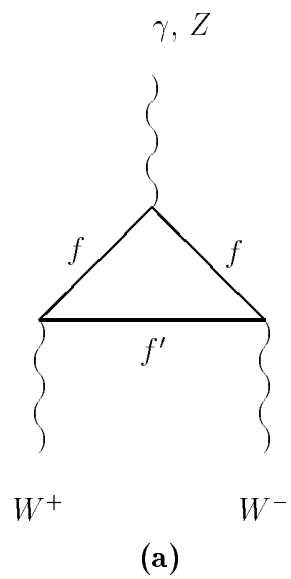


Figure 2

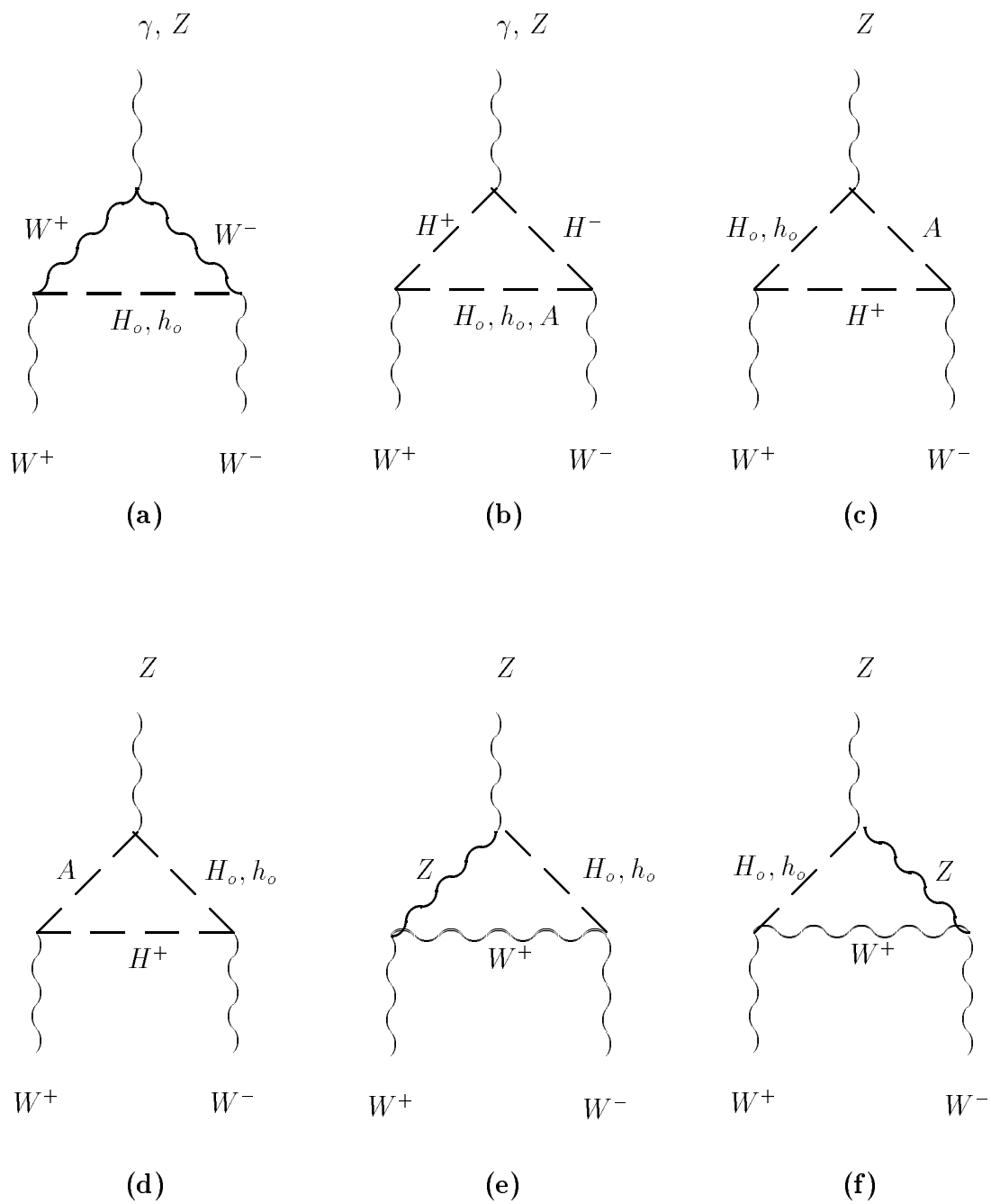


Figure 3